

## **Chapter 6**

# **Magnetic-ordering of polycrystalline Thulium Iron Garnet thin film**

### **abstract**

In the quest to utilize ReIG with perpendicular magnetic anisotropy (PMA) in futuristic spintronics, the attention turned towards iron garnet thin films. Among this family, the one candidate is TmIG that manifests PMA with excellent Gilbert damping, making this material a potential candidate in magnonics devices. This chapter presents a cost-effective deposition approach for TmIG thin films deposited on a thermally oxidized Si(100) substrate. The thin film crystal structure was confirmed with the XRD. The thickness evolution was measured with the XRR, and elemental stoichiometry was confirmed using XPS. Magnetic ordering is observed using SQUID-VSM. The magnetic properties of the thin films indicate a compensation temperature  $\approx 15$  K. This polycrystalline TmIG thin film with low compensation and excellent crystallinity has confirmed the potential of sol-gel-based spin coating as the deposition method.

## 6.1 Introduction

The presence of significant PMA is crucial for stability and higher compactness of the information processing in magnetic materials, along with the low Gilbert damping parameter, which has been demonstrated in rare-earth iron garnet (ReIG) and bismuth substituted YIG [219, 220, 221, 222, 223]. The presence of PMA in ferromagnetic insulators (FMI) opens the application of ReIG in racetrack memory and logic gates [66]. Lower damping, extended magnon decay length, PMA, spin-orbit coupling, and strong spin-mixing conductance in TmIG/Pt hetero-structure indicates its potential application in spintronics [224, 18]. The synthesis of solution-based rare-earth iron garnet is possible. The rare earth has low-temperature ferromagnetic ordering, which affects the net magnetization. As the temperature decreases, its moment aligns opposite to the  $\text{Fe}^{3+}$  magnetic moment, giving rise to compensation temperature. This temperature at which the minimum magnetic moment is observed is known as the compensating temperature of the rare-earth garnets [23]. A low compensation temperature for the TmIG has been predicted in the literature. This chapter presents experimental evidence of low-temperature compensation using DC magnetometry. In previous investigations, TmIG thin films have been grown using rf-sputtering and PLD [219, 220, 221, 222, 223, 34].

This chapter presents an all-aqueous solution-based sol-gel-based spin-coating method to deposit excellent quality TmIG thin films on a thermally oxidized Si (100) substrate. Sol-gel-based spin-coating is a cost-effective way to deposit the oxides [50, 45]. The polycrystalline thin film on thermally oxidized Si(100) has been synthesized. The structural and magnetic properties of the deposited film have been studied using XRD, XRR, AFM, and SQUID-VSM. A low-thickness TmIG sample with moderate roughness has been characterized to confirm its stoichiometry using the XPS. The magnetic properties are discussed using SQUID-VSM. The characterizations confirm that the single-phase,

stable ferrimagnetic insulator with low compensation temperature is useful for magnonic applications as it provides full-range magnetization with high Curie temperature.

## 6.2 Results and Discussion

### 6.2.1 Structural Study

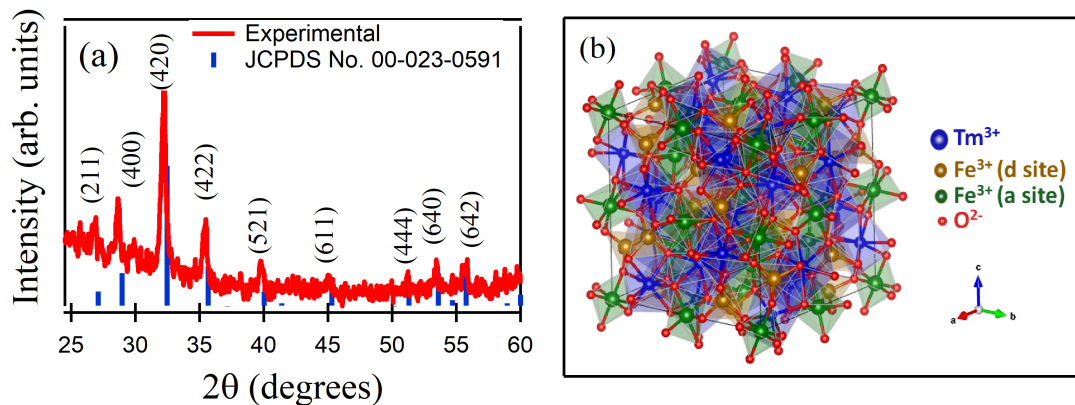


Fig. 6.1 The structural study of the TmIG thin film (a) X-ray diffraction graph of TmIG, (b) unit cell of TmIG.

XRD is a powerful tool for confirming the crystalline state of compounds. Figure (6.1)(a) depicts the diffraction pattern of the TmIG thin film deposited on thermally oxidized Si using the sol-gel process. The structural phase is confirmed using JCPDS file No. 00-023-0591 [225, 226]. The Bragg reflections of all the planes (211), (400), (420), (422), (521), (611), (444), (640), and (642) are distinguishable in the XRD pattern. The XRD confirms the space group  $Ia\bar{3}d$  is a cubic crystal structure. Analysis of the XRD pattern considering (400), (420), (422), and (521) Bragg reflections provides lattice parameters  $a = b = c = 12.4277 \pm 0.0221$  Å. As the crystal structure is cubic, angles are  $\alpha = \beta = \gamma = 90^\circ$ . XRD supports the polycrystalline phase of the deposited thin film. Using Scherrer's equation, the crystallite size was estimated, considering the highest intensity peak of the Bragg plane (420) with full-width half maxima  $0.368 \pm 0.002$  [159]. The crystallite size

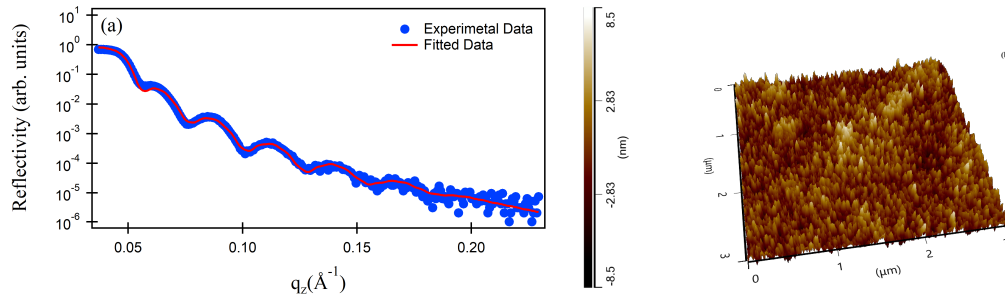


Fig. 6.2 The thickness analysis of the epitaxial TmIG utilizing the (a) XRR and the topography study utilizing the (b) AFM.

can be measured using multiple peaks, but the highest intensity peak was used as the other peaks were not significantly intense. The crystallite size estimated is  $16 \pm 2$  nm. The nanoparticles are arranged on the substrate homogeneously, with surface textures explained in the next section. Figure: (6.1)(b) depicts the crystal structure of the TmIG produced using VESTA software to present the picture of the iron garnet unit cell. The dodecahedral blue  $\text{Tm}^{3+}$  cations with the tetrahedral Golden  $\text{Fe}^{3+}$  cations and green octahedral  $\text{Fe}^{3+}$  cations with the red  $\text{O}^{2-}$  anions. Eight formula units make a unit cell with 160 atoms per unit cell.

### 6.2.2 Topography Study

The non-destructive method to analyze the thickness and roughness is the XRR. XRR is used to analyze the TmIG thin film's thickness and roughness quality. Figure (6.2)(a) depicts the fitted XRR experimental data with Parratt's formalism [110, 208]. The thickness estimated using XRR is  $22 \pm 1$  nm with a surface roughness of  $1.4 \pm 0.1$  nm. The interfacial roughness between  $\text{SiO}_2$  and TmIG is  $0.8 \pm 0.1$  nm. Figure: (6.2)(b) shows the 3-dimensional surface morphology of the TmIG thin film. It concludes the homogeneous surface with a mean roughness of  $1.2 \pm 0.1$  nm, which is the same range as estimated by XRR. The surface is of good quality with moderate roughness.

### 6.2.3 Elemental and ionic environment Study

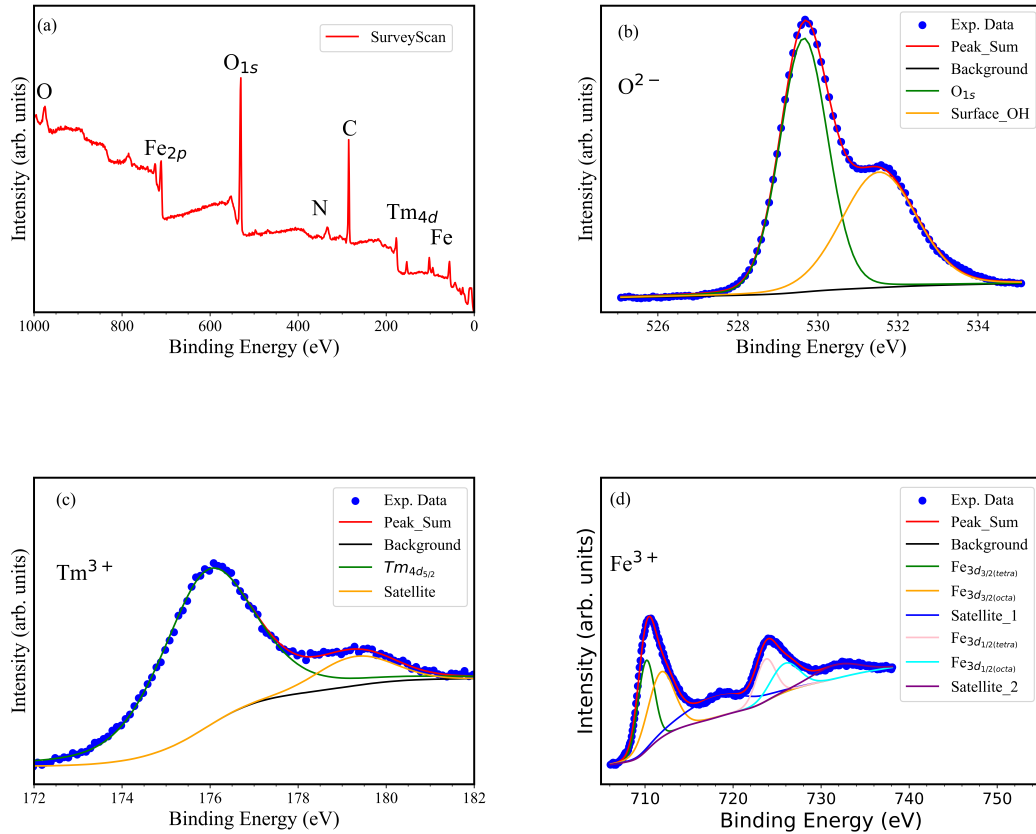


Fig. 6.3 (a) Survey scan of the TmIG sample depicts the presence of elements Fe, O, Tm, and C on the surface. High-resolution spectrum of the (b)  $O_{1s}^{2-}$ , (c)  $Tm_{4d}^{3+}$ , and (d)  $Fe_{2p}^{3+}$  is deconvoluted.

XPS is a nondestructive technique to probe the stoichiometry of the deposited thin film. Figure (6.3)(a) shows a survey XPS scan of the deposited thin film. It verifies the presence of thulium, iron, oxygen, carbon, and nitrogen. XPS is calibrated with a carbon peak at  $285.0 \pm 0.1$  eV, higher than the literature value of 284.5 [227] eV with a difference of 0.5. Figure (6.3)(b) is a high-resolution spectrum of the  $O_{1s}$  with a peak at  $529.6 \pm 0.1$  eV coexisted with the sister peak at  $531.5 \pm 0.1$  eV.  $O_{1s}$  is the bulk contribution of the TmIG, and the sister peak is the result of the surface oxygen and hydroxyl environment

at the top. Figure (6.3)(c) depicts high-resolution spectrum of the  $\text{Tm}_{4d_{5/2}}$ . The peak of  $\text{Tm}^{3+}$  ion in the spectrum is at binding energy  $175.9 \pm 0.1$  eV, which is 0.5 eV higher than the value  $175.4 \pm 0.1$  eV present in the XPS database for the  $\text{Tm}_{4d_{5/2}}$  [227]. The presence of a satellite peak depicts the 3+ cationic state of the Thulium [228, 229]. Figure (6.3)(d) is a high-resolution spectrum of the  $\text{Fe}_{2p}$  orbital. There are two different kinds of Fe environments. First is tetrahedral ( $\text{Fe}_{tetra}$ ) and second is octahedral ( $\text{Fe}_{octa}$ ). The deconvolution of the  $\text{Fe}_{2p}$  gives the these contributions distinctively. The ratio of the intensity of  $I_{\text{Fe}_{octa}}$  and  $I_{\text{Fe}_{tetra}}$  of  $\text{Fe}_{2p_{3/2}}$  spectrum is 0.71 and  $\text{Fe}_{2p_{3/2}}$  spectrum is 0.61, the average of both gives 0.66 which is equivalent to the theoretical value 2:3. The presence of satellite peak at  $\approx 8$  eV from the tetrahedral environment confirms the presence of  $\text{Fe}^{3+}$  ion, as present in literature [167, 50]. The atomic percentage analysis using the XPS has been performed using CasaXPS software [169]. The thulium, iron, and oxygen are present in 12%, 26%, and 62%, respectively, are very close to the desired TmIG stoichiometry ratio 3:5:12. The atomic percentage analysis confirms the purity of composition and the absence of any secondary phase in the deposited thin film.

#### 6.2.4 Magnetic Study

The magnetic study of the TmIG is essential to know its magnetic ordering. The literature suggests a low-temperature compensation in TmIG bulk of 14 K [23]. This work used SQUID-VSM to study room temperature and low-temperature magnetization behavior of TmIG. Figure (6.4)(a) depicts the magnetization as a function of the temperature  $M(T)$  curve in the presence of a 10 mT magnetic field of TmIG thin film.  $M(T)$  curve follows the trend of the bulk TmIG as reported in literature [15, 23]. With the decrease in temperature, magnetization increases until 173 K and then decreases as temperature reduces further to 15 K, where it shows a minimum and increases further. Magnetization supports the bulk-like magnetic ordering of the TmIG on the thermally oxidized Si (100) synthesized

using the complete solution method. The reduction in the magnetization at 173 K is due to antiferromagnetic coupling and the complex moment canting behavior of Tm cations with the tetrahedral and octahedral Fe cations as represented in the Figure (1.2) (b). It shows the schematic of the competition of the moment of iron and thulium present in the system, which is inspired by the compensation mechanism explained by Wang *et al.* [225]. The structure of TmIG gives information that there are two species of the  $\text{Fe}^{3+}$  ions: one is octahedral (a-site), and another is tetrahedral (d-site). These two  $\text{Fe}^{3+}$  cations have antiferromagnetic coupling as supported by the Figure (6.4)(a). In dodecahedral rare-earth  $\text{Tm}^{3+}$  ion, moment starts to originate with paramagnetic to antiferromagnetic ordering below 56 K and modulated ferromagnetic order below 32 K [230]. The competition between the dodecahedral  $\text{Tm}^{3+}$  and tetrahedral and octahedral  $\text{Fe}^{3+}$  is a result of the canted magnetic moment of different sites as depicted in Figure (6.4)(b). The literature proposed that the temperature dependence of the magnetization of thulium metal shows the highest magnetic moment across  $\approx 15$  K [231]. These competing moments at which they are opposite to each other and moment of  $\text{Tm}^{3+}$  at maxima give rise to the minima in the  $M(T)$  plot (the compensation temperature at  $\approx 15$ K) and further increase at the moment due to the enhancement of the moment of Fe and decrement in the moment of Tm at lower temperature. This low-temperature compensation goes hand in hand with literature value [23]. The presence of transition near 50 K is due to the oxygen leakage in the chamber of the MPMS [232]. The oxygen absorbed at the surface due to lower temperatures on the substrates, and as the sample size was a few  $\text{mm}^2$ , the moment was less order of  $10^{-5}$ , giving rise to this transition in the plot and literature well-established this transition to be anti-ferromagnetic [233, 234, 235].

Figure (6.4) (c) and (d) shows magnetic hysteresis of TmIG thin film (c) at  $5\text{K} < T_{comp}$ , and (d) at  $300\text{K} \gg T_{comp}$ . The magnetic hysteresis at 5 K gives the signature of the two competing ferromagnetic ordering. The kink in the magnetic hysteresis is because of the

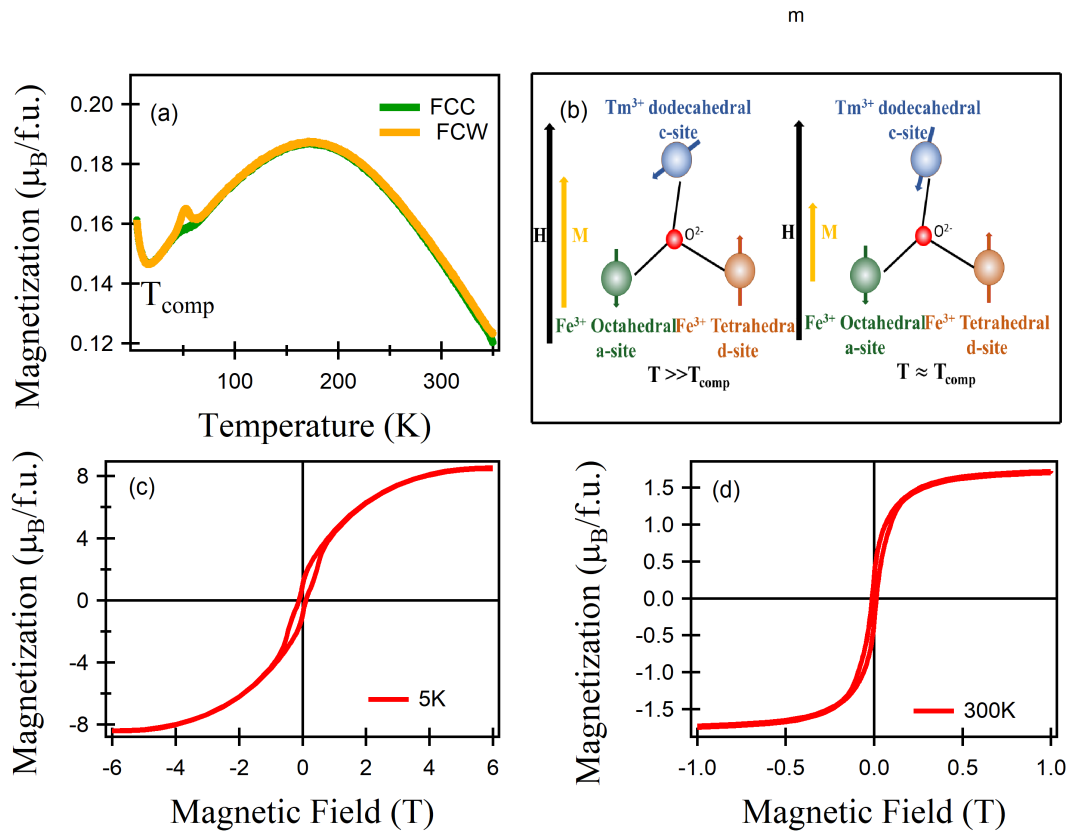


Fig. 6.4 (a) Magnetization as a function of the temperature of the TmIG at 10 mT, (b) Schematic of the moments a-site, d-site, and c-site above the compensation temperature and at the compensation temperature, and (c) and (d) are the in-plane magnetic hysteresis of the TmIG at 5 K and 300 K, respectively.

two competing magnetic lattices of  $Tm^{3+}$  and the  $Fe^{3+}$ . Two different contributions to the hysteresis overlap and give net magnetization as a function of an external field, resulting from this kink. The saturation moment is  $\approx 8 \mu_B/f.u.$  at 5 K. Figure (6.4)(d) depicts the room temperature magnetic hysteresis. The saturation magnetization was calculated by averaging the positive and negative value of the saturation of the TmIG hysteresis at 300 K, giving a saturated moment of  $1.7 \mu_B/f.u.$  for the room-temperature ferrimagnetic coupling [236]. A magnetic coercivity of 12.6 mT is observed. The magnetic order of the TmIG thin film on thermally oxidized Si (100) is a canted ferrimagnetic, similar to the bulk. Solution-based spin coating is a cost-effective method to deposit the rare-earth garnets

showing similar magnetic ordering as its bulk. Both low temperature and room temperature behavior are present.

### 6.3 Summary

TmIG thin film of  $22 \pm 1$  nm thickness has been successfully deposited using a sol-gel-based spin coating. The nature of the thin film is polycrystalline, and it is a homogeneous thin film with roughness  $1.4 \pm 0.1$  nm. XPS confirms the stoichiometry is maintained and the presence of  $\text{Tm}^{3+}$ ,  $\text{Fe}^{3+}$ , and  $\text{O}^{2-}$  ions in the sample. Magnetic measurement supports the complex magnetic nature of the ferrimagnetic coupling with  $\approx 15$  K as compensation temperature of the deposited sample. The hysteresis curve shows the low-temperature modulated ferromagnetism with the room-temperature ferrimagnetic ordering.